Received: 25 March 2024 | Accepted: 6 September 2024

DOI: 10.1002/csc2.21377

Crop Science

ORIGINAL ARTICLE

Special Section: 2025 International Turfgrass Research Conference

A method to spatially assess multipass spray deposition patterns via UV fluorescence and weed population shifts

Daewon Koo | **Navdeep Godara** | **Juan R. Romero Cubas** | **Shawn D. Askew**

School of Plant and Environmental Sciences, Virginia Polytechnic Institute and State University, Blacksburg, Virginia, USA

Correspondence
Shawn D. Askew, School of Plant and Environmental Sciences, Virginia Polytechnic Institute and State University, Blacksburg, VA 24061, USA.
Email: saskew@vt.edu

Assigned to Associate Editor Marco Schiavon.

Funding information
BASF Corporation

Abstract

Spray deposition patterns from agricultural sprayers are traditionally sampled discretely along a field transect accounting for 0.5% or less of the treated area. Such methods may not fully capture the dimensional variability inherent in large-scale, multiple-pass spray applications, especially evident from an agricultural spray drone (ASD). This study investigated the utilization of UV-fluorescent dye and nighttime aerial imaging techniques to assess large-scale, multipass spray deposition patterns. Accuracy of digital hue from UV-fluorescent photography to predict deposition of proxy dye was confirmed via fluorometry assessed intensity levels of extracted UV-fluorescent dye from 384 Petri dishes placed prior to treatment. Results showed that ASD applications, regardless of nozzle type, exhibited greater spatial variability within the target area compared to ride-on sprayer applications, primarily due to overapplication. Additionally, the ASD generated spray drift to adjacent nontarget areas that was at least three times more than that of ride-on and spray-gun sprayers. Multipass deposition was further assessed via in situ smooth crabgrass infestation following treatment with quinclorac or topramezone by multipass ASD or hand-held, four-nozzle spray boom. Weed infestation annotated from overlaid grids with 9.3-dm^2 ground resolution inconsistently detected spatial heterogeneity between transects assessed along the center and edge of each sprayer pass. The ASD controlled smooth crabgrass 11% more than the hand-held sprayer, albeit with an 18% increase in spray drift to nontarget areas, similar to the UV-fluorescence study. Digitally assessed average hue of fluorescence photography appears to be a viable method to assess multidimensional and continuous spatial relationships of spray deposition.

Plain Language Summary

Spraying herbicides evenly is crucial for effective weed control. While the use of agricultural spray drones is increasing, there is limited understanding of their spray uniformity and drift potential. Inconsistent spray patterns can lead to

Abbreviations: ANOVA, analysis of variance; ASD, agricultural spray drone; DAT, days after treatment.

overapplication or under-application, reducing weed control efficacy, or causing unintended crop damage. This study examined how agricultural spray drones, ride-on sprayers, and handheld spray guns distribute herbicides, using UV-fluorescent dye and nighttime imagery or aerial photos to detect weed population shifts. Results showed that ride-on sprayers applied chemicals more evenly, while drones and spray guns had more overapplication, especially with drones spraying too much directly below. Drones also caused more drift, but they achieved better weed control potentially due to fine spray particles covering more weeds. Although drones are less uniform, they can be effective for weed control but pose a higher risk of environmental impact through drift.

1 | INTRODUCTION

Most research related to spray deposition uniformity has been focused on nozzle types and nozzle orientation (Azimi et al., 1985; Grisso et al., 2019; Sumner, 2012). Less is known about large-scale, multipass spray deposition patterns. According to ISO 24253-1, spray deposition sampling in the field was conducted by spraying tracers and capturing the spray with collectors placed in a continuous line in a plane surface (ISO, 2015). Previous researchers have utilized paper-based samplers such as water-sensitive papers (WSP) to assess deposition patterns of water-based sprays (Cunha et al., 2012; Panneton, 2002; Salyani & Fox, 1999; Salyani et al., 2013). Plastic and glass-based samplers such as Mylar cards and Petri dishes are used together with UV-fluorescent dye as a tracer (B. K. Fritz et al., 2011; Wang et al., 2020). These samplers were placed at discrete positions along a transect of the field, often accounting for less than 0.5% of the target area (Qin et al., 2016; Wang et al., 2019). Multiple lines of samplers were added to consider the spatial variability in two dimensions (B. K. Fritz et al., 2011; Wang et al., 2020). The spray deposition pattern in the field was estimated either based on the relative droplet coverage or the tracer quantity. Cotton string, monofilament line, and paper strips have been used together with fluorescent dye to either collect continuous spray deposition pattern or quantify vapor drift (Bae & Koo, 2013; Solie & Gerling, 1985; Wen et al., 2019). Most previous work has sampled less than 0.5-dm^2 areas at large, multi-meter discrete spacing.

Another way that researchers have estimated multipass spray patterns is by characterizing a single pass and simulating additional passes. The mechanical patternator is a widely-used method for researchers and practitioners to assess the spray deposition of one or more nozzles mounted on a spray boom. Patternators generally consist of a series of cylindrical collection tubes evenly spaced which collect the sprayed solution from an array of nozzles (Azimi et al., 1985; Debouche et al., 2000; Ozkan & Ackerman, 1992; R. G. Richardson et al., 1986; Thornton & Kibble-White, 1974). Collected fluid can be either manually or digitally recorded, and the spray uniformity is evaluated by calculating the coefficient of variation (CV) within the targeted spray swath. Though there has been no clear threshold for uniform deposition pattern, arbitrary CV thresholds of 15% for ground sprayers (Prairie Agricultural Machinery Institute, 1989) and 25%–30% for aerial applicators (B. Fritz & Martin, 2020; B. Richardson et al., 2020) have been suggested, considering that the maximum acceptable CV is 30% (Parkin & Wyatt, 1982; B. Richardson et al., 2004).

Large-scale spray deposition uniformity is estimated by simulating the overlapped pattern of measured single-pass deposition (Grift et al., 2000). In actual field applications, however, secondary effects from environmental factors such as wind direction, speed, or topography could alter the spray deposition pattern (B. Fritz et al., 2019; Nordbo et al., 1993; B. Richardson et al., 2020). In addition, the success of pattern simulation will likely be equipment dependent. Agricultural spray drones (ASDs), for example, may not deliver inherently uniform spray patterns due to variable wind generated by the machine during flight (Li, Giles, Andaloro et al., 2021; Teske et al., 2018).

A modern ASD sprays an ultra-low volume and produces a fine spray of droplets prone to movement in variable wind patterns (B. Fritz et al., 2019; Hunter et al., 2020). Previous research has shown that ASD spray deposition patterns are height dependent and prone to evaporative losses when the intended spray height remains between 2 and 10 m above the ground (Koo et al., 2022, 2024). When an ASD was operated within 2 m aboveground, pest control has been equivalent or better than when sprayed via a ground-based applicator (Koo et al., 2023; Li, Giles, Niederholzer et al., 2021; Qin et al., 2016). The pattern deposited by an ASD at 2-m height, however, showed disproportionately large deposition directly under the sprayer compared to that deposited to the outer 30% of the intended spray width (Koo et al., 2024). This increased deposition may improve weed control from single-pass

herbicide treatments on small plots that would be less evident when larger, multipass applications are made as performance of many herbicides is rate dependent (Brewer et al., 2017; Brosnan et al., 2013).

Discrete sampling methods such as WSP and Mylar cards may not adequately assess dimensional variability from large, multiple-pass spray applications. Weed control from multipass ASD applications of herbicides has also not been reported in scientific literature. In this study, a novel technique was developed using UV-fluorescent dye and image analysis techniques to assess large-scale, multipass spray deposition patterns by analyzing deposition quantity to the entire treated area on a 0.27 dm^2 scale following treatment with an ASD sprayer, ride-on sprayer, and a spray gun with flooding nozzle. We hypothesized that deposition uniformity would vary with application equipment. Our first objective was to evaluate the percentage of areas that received overapplication, under-application, and drift across four application scenarios using the aforementioned equipment. Our second objective was to determine weed control efficacy from large-plot, multipass applications of selective herbicides using an ASD sprayer and a CO_2-pressurized handheld boom sprayer and estimate drift and application uniformity based on posttreatment weed population.

Core Ideas

- Traditional spray deposition assessments lack spatial dimensionality.
- Nighttime UV-fluorescence photography of proxy dye accurately assesses spray deposition patterns.
- Spatial heterogeneity and drift increase with agricultural spray drones compared to ride-on sprayers.
- Weed infestation annotated via grid-overlaid aerial images resolves drift more than spatial heterogeneity.
- Despite erratic deposition, spray drones conserve or enhance weed control compared to a handheld boom sprayer.

2 | MATERIALS AND METHODS

2.1 | Assessing multipass spray deposition pattern of various sprayers

Field trials were conducted at the level pavement at the Glade Road Research Facility, Blacksburg, VA (37°13′56.3″ N, 80°26′09.3″ W) between August 2023 and February 2024 as randomized complete block designs. The targeted treatment area in each plot was 8.6-m long and 3.7-m wide and surrounded by a 0.6-m buffer. Each plot also included a 0.6-m × 8.6-m area where known doses of tracer dye were deposited as references (Figure 1). The study was repeated two times, and experimental units were replicated three times per trial.

A fluorescent dye solution (Cartax DP Liquid; Heubach Colorants USA LLC) was applied at 3.7 L ha^{-1} by an ASD sprayer, simulated ride-on sprayer, and spray gun with flooding nozzle (Table 1). A DJI Agras MG-1P (DJI) ASD was commercially equipped with extended-range flat-fan nozzles (TeeJet XR11001; Spraying Systems Co.). The nozzles were arranged as four nozzles on the corners, 1.4 m apart within the row and 0.6 m between the rows, and operated at 2 m above the ground (Figure 2a). The flow rate was maintained at 5.05 mL s^{-1} per nozzle, and the spray volume was specified at 28 L ha^{-1}. Three passes of the ASD were needed to treat the intended area of each plot with a user-selected, 2.8-m spray swath collectively covering the entire 8.5-m-long axis. Spray heights were maintained by a radar sensor mounted on the ASD. In another treatment, the spray nozzle configuration was altered to Venturi-type nozzles (TeeJet AIXR11002; Spraying Systems Co.) spray tips arranged as one nozzle on each side of the ASD with a flow rate maintained at 10.1 mL s^{-1} per nozzle (Figure 2b). Targeted spray swath, spray volume, and spray height were identical in both ASD treatments. A third treatment consisted of a ride-on sprayer that was simulated by retrofitting a zero-turn mower of similar chassis with a boom designed to match the nozzle type, spacing, and height of the ride-on sprayer (SG42; Steel Green Manufacturing). The boom consisted of four Venturi-type nozzles (TeeJet AIXR110025; Spraying Systems Co.) spaced 0.5 m and maintained at 0.5 m above the ground. The sprayer required four passes to treat the intended plot area with 2.1-m line spacing and a spray volume of 140 L ha^{-1}. The fourth treatment included a handheld spray gun with a flooding nozzle (Lesco Chemlawn Spray Gun; SiteOne Landscape Supply) typically used for lawn-care treatments (Butler et al., 2019; Patton et al., 2018). The gun was pressurized by CO_2 gas and calibrated to deliver 1645 L ha^{-1}. The application was conducted by moving the spray gun left to right making approximately 30 parabolic spray patterns in each of two 1.8-m paths down the long axis of each plot. In all cases, the 0.6-m buffer that surrounded each targeted treatment area was used to assess spray drift to a nontargeted area (Figure 1b).

On the reference area located on one edge of each plot, UV-fluorescent dye solution was applied with a CO_2-pressurized sprayer with a four-nozzle spray boom equipped with four flat-fan nozzles of increasing orifice sizes (TeeJet TP8001; TP8002; TP8004; TP8008; Spraying Systems Co.) (Figure 1c). The UV-fluorescent dye was mixed to deliver an intended dose of 3.7 L ha^{-1} at 373 L ha^{-1} total spray volume based on preliminary studies that assessed UV fluorescence of spray patterns. The actual output from each nozzle that was delivered during the study was targeted 0.25, 0.5, 0.95, and 1.9

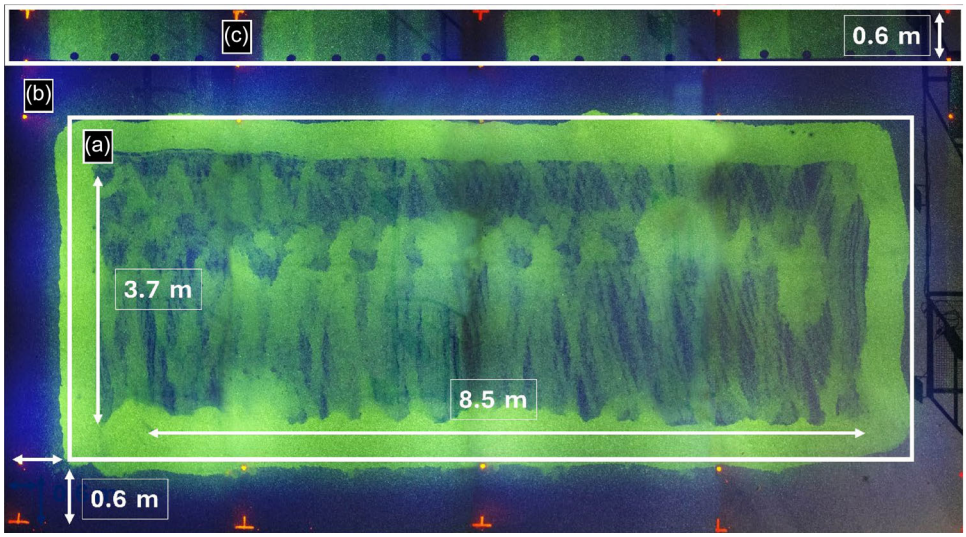

FIGURE 1 Plot design on the level pavement at the Glade Road Research Facility where (a) the target area of 3.7-m wide and 8.5-m long, (b) the nontarget buffer area of 0.6-m surrounding the target area, and (c) the reference area of 0.6-m wide strips where nominal UV-fluorescent dye rates of 0.25, 0.5, 0.9, and 1.9 times of the intended rate were applied by four-nozzle spray boom equipped with different sizes of flat-fan nozzles. *Note*: Multipass application was perpendicular to the 8.5-m-long axis with three passes with 2.8-m targeted swath (spacing) for analysis of variance (ASD) applications, and four passes with 2.1-m targeted swath (spacing) for ride-on sprayer. For the spray gun application (shown), 30 parabolic passes of spray in each 1.8-m two paths widthwise along the treated plot inside the perimeter spray followed by the application on the perimeter of the targeted treatment area.

TABLE 1 Sprayer devices and application parameters for a study assessing UV-induced fluorescence of a tracer dye delivered in multiple passes by four devices.

Sprayer device[a]	Spray volume (L ha^{-1})	Fluorescent dye concentration (% v/v)	Passes (No. plot^{-1})	Swath width (m)	Application height (m)	Speed (km h^{-1})
DJI MG-1P + XR11001	28	13.3	3	2.8	2.0	8.8
DJI MG-1P + AIXR11002	28	13.3	3	2.8	2.0	8.8
Spray gun + flooding nozzle[b]	1645	0.23	40	0.5	1.0	4.5
Ride-on sprayer + AIXR110025	140	2.7	4	2.1	0.5	7.5

[a]UV-fluorescent dye ratio was calibrated to deliver 3.7 L ha^{-1} regardless of the sprayer type.
[b]Perimeter of the targeted treatment area was sprayed first followed by 30 parabolic passes of spray in each of two paths lengthwise along the treated plot inside the perimeter spray.

times the intended dose from left to right on the boom. These four doses were treated on the border of each quadrant of each plot (four dose–response sets per experimental unit) because the imaging system could only record one-fourth of the plot area due to limitations in achieving uniform UV light illuminance (Figure 1c). Petri dishes (KIMBLE KIMAX, DWK Life Sciences) with inner diameter of 100 mm were placed during the application under each nozzle path. Petri dishes were collected, treated with 5 mL of *N*, *N*-dimethylformamide solution (Spectranalyzed, Thermo Fisher Scientific), and shaken at 150 rpm with a G2 Gyratory Shaker (New Brunswick Scientific Co.) for 10 min. Afterward, 45 mL of tap water was added to the UV-fluorescent dye-extracted solutions and stirred 100 times with the micropipette tip (Finnpipette Digital ACL 200–1000 µL, Thermo Fisher Scientific). A 2 mL aliquot of extract was removed from Petri dishes, and the fluorescence intensity was measured with a QE Pro spectrometer (Ocean Insight). UV-fluorescent dye contents in each Petri dish were estimated based on Equation (1) which was derived from the standard curve between known Cartax DP Liquid rate (R_k) in L ha^{-1} and fluorescence intensity (f). The standard curve was based on a preliminary experiment where 11 different concentrations of Cartax DP Liquid were delivered via track sprayer at constant application volume, which was confirmed via weight of spray solution in Petri dishes that were subjected to similar extraction and UV fluorescence intensity measurement ($R^2 = 0.99$).

$$R_k = 0.0077 f. \quad (1)$$

A portable structure was mounted with six 50-W, 365 nm ultraviolet lamps (Everbeam) such that three lights were spaced 1.8 m apart on each of two axes spaced 2.4 m apart to uniformly illuminate a 2.4-m wide and 5.5-m long area

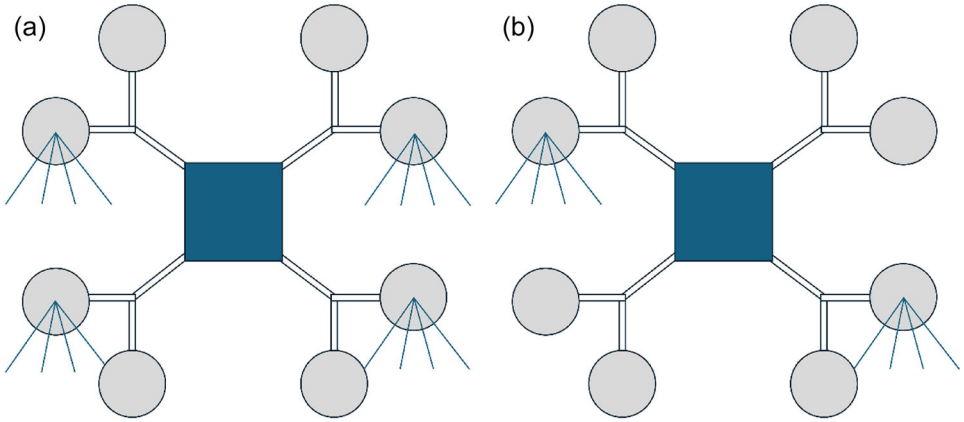

FIGURE 2 Schematic diagram of DJI MG-1P including nozzle and rotor configuration. (a) Four TeeJet XR11001 nozzles were equipped and (b) two TeeJet AIXR11002 nozzles were equipped while one nozzle on each row was blocked to achieve sufficient pressure for nozzles with a larger orifice size.

that comprised one-fourth of each experimental unit. Each illuminated area was photographed at night between 9 p.m. and midnight using a DJI Phantom 4 Advanced (DJI) or DJI Mavic 2 Enterprise (DJI) drone operated at a 5-m height. Each image contained a reference area of four known doses, nontarget border areas of 0.6-m width used to assess spray drift, and targeted treatment area. Each image was overlaid with a 5000-point grid comprising a 0.27-dm^2 resolution using FieldAnalyzer (Green Research Services LLC) to calculate average hue within the image for a total of 20,000 assessments per experimental unit. Each grid point was classified as belonging to the targeted spray area, nontarget drift-assessment area, or the center of each of four reference-dose areas. The average hue in each 0.27-dm^2 grid was converted to estimated UV-fluorescent dye by subjecting the four reference dose areas from each image to the logarithmic Equation (2) and solving for the estimated dose that was deposited in that spatial grid. The relationship of average digitally assessed hue and Cartax DP Liquid rate is given as:

$$R_e = e^{(H/s - I/s)}, \quad (2)$$

where R_e indicates the estimated Cartax DP Liquid rate (L ha^{-1}) in field plots derived from digital hue, e is the natural logarithm, H indicates the average hue value, and S and I are the slope and intercept of a logarithmic equation between R_k and H on the reference area from each image (one-fourth of each field plot). Once all grids were converted to the estimated deposition rate, proportions within the plot that were below 50% and over 150% of the targeted dose rate of 3.7 L ha^{-1} were calculated to assess under- and overapplication, respectively. The area between 50% and 150% of the targeted dose rate was considered acceptable. Also, the proportion of dose rate over 50% of 3.7 L ha^{-1} on the buffer area was calculated to evaluate overspray or drift potential. The calculated areas below and above target rate and nontarget deposition were subjected to analysis of variance (ANOVA) in SAS 9.4 (SAS Institute Inc.) PROC GLM with sums of squares partitioned to reflect replication, trial, treatment, and trial by treatment effects and interactions. The mean square associated with treatment was tested with the mean square associated with the interaction of treatment with the random variable trial. Appropriate main effects or interactions were separated by Fisher's protected least significant difference (LSD) at $\alpha = 0.05$.

2.2 | Multipass deposition estimate based on in situ response of smooth crabgrass to herbicides

Field trials were conducted to estimate magnitude and uniformity of herbicide deposits to targeted areas and drift to nontargeted areas via smooth crabgrass [*Digitaria ischemum* (Schreb.) Schreb. Ex Muhl.] infestation levels following herbicide treatment. Separate trials were initiated on June 15 and July 20, 2023, at the Glade Road Research Facility in Blacksburg, VA, on Dress Blues Kentucky bluegrass (*Poa pratensis* L.) fairways (37°13′50.8″ N, 80°26′12.2″ W) and L93 creeping bentgrass (*Agrostis stolonifera* L.) fairways (37°13′58.4″ N, 80°26′10.7″ W) maintained at 1.5-cm height, respectively. Trials were arranged in randomized complete block factorial designs with two levels of application device, two levels of herbicide, and four replications. Treatments included topramezone at 37 g a.e. ha^{-1} (Pylex, BASF Corporation) and quinclorac at 841 g a.e. ha^{-1} (Drive XLR8, BASF Corporation) applied with the aforementioned ASD sprayer or a CO_2-pressurized backpack sprayer. 0.5% v/v and 1% v/v methylated seed oil adjuvant was added to topramezone and quinclorac application, respectively. Plots were 9.1-m wide and 9.1-m long with a 3-m nontarget buffer

around the perimeter for the ASD application, whereas ground application plots were 7.3-m wide and 7.3-m long with 0.3-m nontarget, perimeter buffer. Nontreated checks included two 0.3-m wide by 1.2-m long rectangles within each plot achieved by covering areas with plywood during the herbicide application.

A DJI Agras MG-1P (DJI) ASD, which was equipped with four extended-range flat-fan nozzles (TeeJet XR11001; Spraying Systems Co.), was used for the ASD application (Figure 2a). All applications were conducted using the manual plus mode which is a semiautonomous application fixing the application parameters and flight direction offered by the controller of the ASD sprayer. Spray volume was set to 28 L ha^{-1} and the application speed was maintained at 6.1 km h^{-1}. The flow rate was maintained at 5.4 mL s^{-1} per nozzle targeting a 3-m spray swath. Spray heights were maintained at 2 m above the ground. The aerial applications were conducted in a back-and-forth pattern for a total of three passes, each with 3-m shift between each pass to ensure the uniform spray coverage across each plot.

A CO_2-pressurized backpack sprayer with a handheld four-nozzle boom equipped with Venturi-type nozzles (TeeJet TTI11006; Spraying Systems Co.) was used for the ground application to simulate spray equipment used for turfgrass weed control (Shepard et al., 2006). The spray boom was placed 0.5 m above the ground to maintain a 1.8-m swath and spray volume was targeted to 373 L ha^{-1}. The ground applications were conducted in a back-and-forth pattern for a total of four passes with 1.8-m shift between each pass to ensure the uniform spray coverage across each plot.

Smooth crabgrass infestation within the targeted treatment area and nontarget buffer area was identified by analyzing aerial images of plots taken by a DJI Phantom 4 Advanced (DJI, Shenzhen, China) imaging drone. A grid of 9.3-dm^2 resolution was overlaid onto each digital image, and each grid position was visually annotated as either "infested" or "not infested" by smooth crabgrass. The ratio of grid positions infested with smooth crabgrass in targeted treatment areas and nontarget buffers was converted to a percentage reduction of average infestation in nontreated checks. Reductions in infestation compared to the nontreated checks in targeted treatment areas were considered "weed control." In the nontargted buffer areas, reductions in smooth crabgrass infestation compared to the nontreated turf were attributed to spray drift. Among the buffer area, 0.6- and 0.3-m periphery outside of the target area was assessed for ASD and CO_2-pressurized backpack sprayer plots, respectively. To assess uniformity of spray patterns, two 0.6-m-wide transects were assessed for smooth crabgrass infestation reduction for each pass of the spray equipment in each plot with previously described methods. These spatially different transects were aligned with the center and edge of each spray pass, and the percentage difference between these two infestation-reduction values indicates uniformity of spray pattern. Larger positive integers of "spatial difference" indicate that smooth crabgrass populations were reduced by a greater percentage under the center of the sprayer compared to the edge.

Data were collected 14 and 28 days after the treatment, but only 28 days after treatment (DAT) data are presented due to similarities between the two assessments. Data were subjected to ANOVA in SAS (SAS Institute) PROC GLM with sums of squares partitioned to reflect replication, trial, device, herbicide, and interactions thereof. The mean square associated with device, herbicide, and device × herbicide was tested with the mean square associated with the interaction of trial with each of these terms (McIntosh, 1983). Data were presented separately by trial if significant trial interactions occurred, otherwise, data were pooled over trial. Appropriate main effects or interactions were separated by Fisher's protected LSD at $\alpha = 0.05$.

3 | RESULTS AND DISCUSSION

3.1 | Assessing multipass spray deposition pattern of various sprayers

The under-applied area was insignificant across all main effects and interactions of the model (Table 2). Under application in the targeted area averaged 12% across all four application devices, trials, and replicates (data not shown). Since this is the first study to parse deposition uniformity spatially between over and under a targeted dose, the reason that under-application was consistent across devices is unclear. It is possible that deposition disparities rarely reach our set threshold deficiency of 50% of the targeted rate when spray is applied by these devices, or our resolution of 0.27 dm^2 may have underestimated or overestimated disparities for all devices. Our resolution is lower and sampled area is higher than previous studies that measured field deposition via larger 0.75 dm^2 WSP that sampled discrete areas comprising approximately 1% of the area sampled (Qin et al., 2016; Wang et al., 2019).

The device × trial interaction was significant for the percentage of targeted treatment area that was overapplied (Table 2). This interaction was likely caused by changes in separation between the two drone applications and the spray gun between years. In 2023, the ASD equipped with XR11001 nozzles deposited more than 1.5 times the targeted dose on 71% of the targeted area and more than all other devices (Table 3). In 2024, however, both ASD applications and the spray gun deposited an overapplication on at least 61% of the targeted area with no differences between these three devices. The ride-on sprayer consistently applied an overapplication of not more than 47% and equivalent to the least amount of overapplication each year (Figure 3D; Table 3). The reason for

TABLE 2 Analysis of variance for studies assessing area of multipass spray deposition based on reflectance and in situ smooth crabgrass infestation.

Deposition study[a]	Under-application	Overapplication	Acceptable application	Drift
Replication	NS	NS	NS	NS
Device	NS	NS	*	***
Trial × device	NS	*	NS	NS

Crabgrass study 28 DAT[b]	Targeted crabgrass control	Infestation after drift	Spatial difference
Replication	NS	NS	NS
Herbicide	NS	NS	NS
Device	*	*	NS
Herbicide × device	NS	NS	NS
Trial × herbicide	NS	NS	NS
Trial × device	NS	NS	**
Trial × herbicide × device	NS	NS	**

Abbreviations: ASD, analysis of variance; DAT, days after treatment.

[a]UV-fluorescent dye was assessed via nighttime imaging with UV lamps and quantified at 20,000 grid sites per plot to assess percentage area that was 50% "under" or 50% "over" the targeted rate, within the "acceptable" rate range, or drifted to nontarget areas at 50% or more of the target rate.

[b]A digital grid of 676 and 1122 squares per plot for ASD and CO_2-pressurized backpack sprayer, respectively, was overlaid on aerial images and smooth crabgrass infestation was assessed by visually counting infested grid sites. These data were converted to a percentage reduction compared to nontreated check plots expressed as "control," infestation reduction compared to the nontreated following drift to nontarget border areas, and the spatial difference between percentage infestation in transects along the center and edge of each sprayer pass.

P values are indicated as NS = not significant or $P > 0.05$, $*P < 0.05$, $**P < 0.01$, and $***P < 0.001$.

TABLE 3 Influence of sprayer type on area of spray deposits in a targeted spray area estimated as overapplied or within an acceptable rate range and area with significant drift to nontarget border areas.

	Over (% area)			
Sprayer device	2023	2024	Acceptable (% area)	Drift (% area)
Spray drone + XR11001	71A	66AB	22B	54A
Spray drone + AIXR11002	49B	61AB	34B	54A
Spray gun	46BC	79A	23B	6B
Ride-on sprayer	27C	47B	49A	17B

Note: UV-fluorescent dye was assessed via nighttime imaging with UV lamps and quantified at 20,000 grid sites per plot to assess percentage area that was 50% "under" or 50% "over" the targeted rate, within the "acceptable" rate range on the target area, or drifted to nontarget areas at 50% or more of the target rate. Under application averaged 12% regardless of sprayer type or trial. Means followed by the same letter within a given column are not different according to Fisher's Protected LSD test at $\alpha = 0.05$.

the increase in overapplied area by the ASD equipped with AIXR11002 nozzles between years is unknown, but other researchers have reported variable deposition between flights, albeit uncharacterized with respect to deposition quantity (Ahmad et al., 2020; Martin et al., 2019).

Slight changes in how the spray gun treatments were applied between years may have contributed to inconsistencies in overapplication from that device. Care was taken each year to hold the spray gun exactly 1.0 m above the ground, but the gun was aimed perpendicular to the ground during the perimeter pass in 2023. Following completion of the study in 2023, it was obvious in the observed patterns that the perimeter pass received more spray than the parabolic swipes of the gun (Figure 3c), as the later was oriented at an approximately 30° angle to the ground. In 2024, the 30° angle was used for both the perimeter pass and the parabolic swipes, apparently increasing the amount of product that overlapped closer to the center of each plot. Such application inconsistency is likely inherent to the spray gun as user-induced changes can dramatically impact the deposition pattern. It is well documented that spray gun applications tend to show less homogeneous spray results compared to spray booms (Foqué et al., 2012; Langenakens et al., 2002; Sánchez-Hermosilla et al., 2011).

The main effect of device was significant ($p < 0.05$) for acceptable deposition in the targeted area and not dependent on trial (Table 2). Specifically, 49% of the target area was classified as acceptable application from the ride-on sprayer, while 22%, 34%, and 23% of the target area came from the ASD sprayer with flat-fan nozzles, the ASD sprayer with air-induction nozzles, and the spray gun, respectively (Table 4). Low deposition uniformity from the ASD and spray gun was expected based on previous reports (Ahmad et al., 2020;

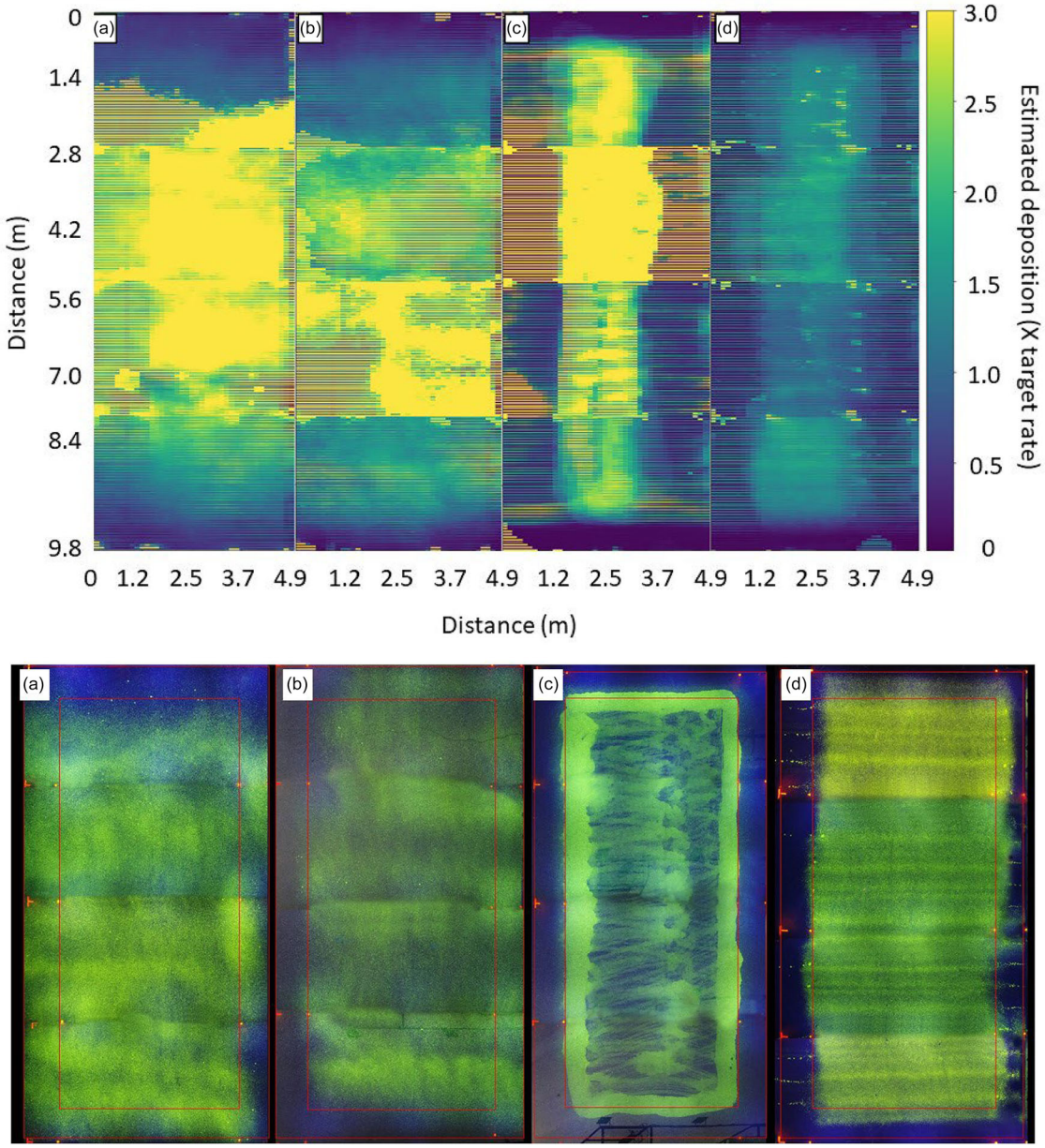

FIGURE 3 Heatmap (top) of fluorescent dye deposition averaged over replicates and trials and mosaiced images (bottom) of selected plots following multipass application by (a) DJI MG-1P + TeeJet XR11001, (b) DJI MG-1P + TeeJet AIXR11002, (c) spray gun + flooding nozzle, and (d) ride-on sprayer + TeeJet AIXR110025. Center (red lines in lower photographs) is a targeted plot, and 0.6-m perimeter is nontarget buffer area to assess drift. Heatmap generated by Python 3.9 using numPy and matplotlib packages.

Foqué et al., 2012; Koo et al., 2024; Langenakens et al., 2002; Martin et al., 2019; Sánchez-Hermosilla et al., 2011). The ride-on sprayer, however, was expected to deliver accurate deposition on more than 49% of the treated area. Upon further investigation, we concluded that the boom height and nozzle spacing, each at 0.5 m, specified by the manufacturer was too high for optimal ground deposition based on visually assessing the drying patterns of water on hot pavement (data not collected) compared to the UV-fluorescence photography (Figure 3d). Although speculative, we believe that streaks of overapplication were caused by excessive spray overlap between nozzles. Regardless, the ride-on sprayer still deposited an accurate dose on over twice as much area as either the ASD with XR11001 nozzles or the spray gun (Table 1), and this effect is evident in the heat map response averaged over replicates and trials (Figure 3).

The main effect of application device was significant ($p < 0.05$) for the percentage of nontarget buffer area that received drift of at least half of the target rate (Table 2). This response was also not dependent on trial (Table 2). Both ASD applications delivered drift to 54% of nontargeted buffer areas and considerably more than that of the spray gun or ride-on

TABLE 4 Influence of two sprayer devices and two herbicides on targeted smooth crabgrass control, reduction in smooth crabgrass infestation after potential drift to nontarget border areas, and spatial difference in smooth crabgrass infestation levels between transects along the center or edge of each sprayer pass following multipass spray applications to weed-infested turf.

	Targeted (%)	Reduction (%)	Spatial difference[b] (%)	
Sprayer device	Crabgrass control[a]	After drift[a]	Topramezone	Quinclorac
Spray drone + XR11001	79A	31A	24A*	2A*
Backpack sprayer	68B	13B	0B	2A

Note: Means followed by the same letter within a given response or level of herbicide are not different according to Fisher's Protected LSD test at $\alpha = 0.05$.

Abbreviations: ASD, analysis of variance; LSD, least significant difference.

[a]A digital grid of 676 and 1122 squares per plot for ASD and CO_2-pressurized backpack sprayer, respectively, was overlaid on aerial images and smooth crabgrass infestation was assessed by visually counting infested grid sites. These data were converted to a percentage reduction compared to nontreated check plots expressed as "weed control," infestation reduction compared to the nontreated following drift to nontarget border areas, and the spatial difference between percentage infestation in transects along the center and edge of each sprayer pass.

[b]Spatial difference exhibited a trial × device × herbicide interaction, but all means were less than 5% in trial 1 with no differences. Thus, only trial 2 data are shown.

*significant difference between herbicides within a given level of device.

sprayer (Table 3). It has been well documented that spray drift increases with higher application height (Bode et al., 1976) and finer droplet size (Butler Ellis et al., 2002; Miller et al., 2011; Stainier et al., 2006; Taylor et al., 2004). The ASD application with flat-fan nozzles produced smaller droplets ranging from "fine" to "very fine" compared to the ride-on sprayer, which generated droplets categorized as "medium" to "extremely coarse" (ASABE, 2020; Spraying Systems Co., 2023). Moreover, the ASD was operated at a height of 2 m versus 0.5 m above the ground for the ride-on sprayer. However, the replacement of flat-fan nozzle to air-induction nozzle for ASD application failed to mitigate drift, which was found to be effective for drift reduction in a wind tunnel study (Alves et al., 2017). Wind generated from rotors of the ASD sprayer might offset the drift reduction effect from the coarser droplet size. In addition, the close proximity of drift assessment relative to the targeted spray area may not allow for adequate separation as occurred in wind tunnel studies over a 2-m distance (Alves et al., 2017). Nozzles with larger orifice may generate even coarser droplets, but the ASD sprayer used in this study does not have enough pump capacity to make this adjustment (DJI, 2018).

3.2 | Multipass deposition estimate based on in situ response of smooth crabgrass to herbicides

The main effect of device was the only significant ($p < 0.05$) effect for the smooth crabgrass control and smooth crabgrass infestation after potential drift to the buffer area at 28 DAT (Table 2). When averaged across herbicides and trials, treatments applied by ASD controlled smooth crabgrass by 79%, which is 11% more than the control achieved with the backpack sprayer (Table 4). Improved smooth crabgrass control by the ASD (Table 4), despite variable deposition patterns detected by digital analysis of UV-fluorescent photography (Table 3), may be attributed to improved weed coverage from fine to very fine spray particles (Knoche, 1994).

Smooth crabgrass infestation reduction following drift to buffer areas was 31% for the ASD and 13% for the backpack sprayer (Table 4). These data strongly support the evidence of increased drift by ASD applications observed following treatment with UV-fluorescent dye (Table 3). Other researchers have also demonstrated increased spray drift by ASD applications compared to ground applications (B. K. Fritz et al., 2011; Wang et al., 2019).

The trial-by-herbicide-by-device interaction was significant ($p < 0.05$) for the spatial difference of smooth crabgrass infestation between the center and the edge of the spray path at 28 DAT. The trial interaction occurred because the first trial had a light wind of 1.6–4.8 km h^{-1} and one-tiller crabgrass compared to no wind and two- to three-tiller smooth crabgrass in the second trial. In the windy environment of the first trial, weed infestation reduction did not vary by more than 5% between transects in the center and edge of each equipment pass with no differences between treatments (Table 4, footnote). Variable wind patterns may have reduced the distinction between spray deposited under the ASD and that deposited on the edge of each pass. In work conducted in a windless environment, deposition between the center and edge of drone passes varied considerably (Koo et al., 2024). Researchers suggested that wind can strongly influence ASD deposition patterns by shifting the pattern downwind of the intended path (B. Fritz et al., 2019; Wang et al., 2019). In the calm conditions with larger smooth crabgrass of the second trial, the distinction between weed population reduction in the center and edge of each pass was more evident but herbicide and application device dependent. Topramezone applied by the ASD in trial 2 reduced smooth crabgrass infestation 24% more in the center of each pass compared to the edge, but either herbicide applied by ground sprayer or quinclorac applied by the ASD did not differ more than 2% between the center and edge of each pass (Table 4).

Smooth crabgrass response from topramezone varies with application rate. Elmore et al. (2012) observed 53% and 47% smooth crabgrass control from topramezone at 9 g a.e. ha^{-1} at 28 and 42 DAT, respectively. Brewer et al. (2017) reported 78%, 87%, and 94% smooth crabgrass control from topramezone application at 18, 37, and 55 g a.e. ha^{-1} at 42 DAT. Brosnan et al. (2013) observed a disparity of smooth crabgrass control from topramezone at 12 and 25 g a.e. ha^{-1} between trial sites, though the trend of increased smooth crabgrass control and topramezone rate remained. However, smooth crabgrass control with quinclorac may not solely depend on the rate response. Previous researchers have extensively discussed the abnormal relationship between the growth stage of smooth crabgrass and its control following quinclorac application. Dernoeden (2001) and Dernoeden et al. (2003) noted variable results in smooth crabgrass control with quinclorac at an application rate of 0.84 kg a.e. ha^{-1} when the growth stage of smooth crabgrass ranged between three leaves and four tillers. Conversely, in other studies, quinclorac at the same rate effectively controlled smooth crabgrass (>98%) regardless of growth stages ranging from one leaf to over three tillers at four weeks after treatment (Brosnan et al., 2010; Putri et al., 2024). Poor performance of quinclorac was more likely to be observed in heavily infested areas.

4 | CONCLUSIONS

Our data suggest that ride-on sprayers with fixed spray booms deposit more uniform and accurate spray than an ASD or spray gun sprayer. The ASD deposits more spray drift to nontarget areas than either the ride-on sprayer or spray gun. Using UV-fluorescent tracer dye and nighttime drone imagery was a useful method to investigate continuous, multidimensional deposition patterns at fine resolution via digital image analysis of average hue. Standard curves relating average digital hue and fluorometrically assessed intensity were both highly correlated to known UV-fluorescent dye doses applied to reference areas via nozzles of varying output. Weed infestation levels assessed via grid counts were less effective at discerning variations in predicted deposition between the center and edge of each spray pass, likely due to variable weed populations inherent to large plots (Cardina et al., 1997). Weed infestation levels suggest that targeted weed control from an ASD can exceed that of a ground sprayer. Weed infestation reduction in nontarget areas supports deposition assessments via UV-fluorescent photography in that spray drift by an ASD can be several times greater than that of a ground sprayer.

AUTHOR CONTRIBUTIONS

Daewon Koo: Conceptualization; data curation; formal analysis; investigation; methodology; software; visualization; writing—original draft. **Navdeep Godara**: Data curation; investigation; software; writing—review and editing. **Juan R. Romero Cubas**: Investigation; writing—review and editing. **Shawn D. Askew**: Conceptualization; data curation; formal analysis; funding acquisition; investigation; methodology; supervision; writing—review and editing.

ACKNOWLEDGMENTS

The authors thank Heubach Colorants USA LLC for donating Cartax DP Liquid and Dr. Dale Sanson, Senior Director of Formulation Development and Compliance Chemistry, PBI Gordon Corporation for initial discussions regarding UV-fluorescent tracer dyes. The authors also thank BASF corporation for donating topramezone and quinclorac herbicide and for partially funding this research. The technical support of Jeremy Leichner is also appreciated. This research was partially funded by BASF Corporation and based on a request to "determine the viability of ride-on sprayers and spray drones for pest control in turfgrass."

CONFLICT OF INTEREST STATEMENT

The authors declare no conflicts of interest.

ORCID

Daewon Koo https://orcid.org/0000-0001-5055-7307
Navdeep Godara https://orcid.org/0000-0002-1452-5225
Juan R. Romero Cubas https://orcid.org/0009-0002-7456-0054
Shawn D. Askew https://orcid.org/0000-0002-9515-9502

REFERENCES

Ahmad, F., Qiu, B., Dong, X., Ma, J., Huang, X., Ahmed, S., & Chandio, F. A. (2020). Effect of operational parameters of ASD sprayer on spray deposition pattern in target and off-target zones during outer field weed control application. *Computers and Electronics in Agriculture*, *172*, 105350. https://doi.org/10.1016/j.compag.2020.105350

Alves, G. S., Kruger, G. R., da Cunha, J. P. A., de Santana, D. G., Pinto, L. A. T., Guimarães, F., & Zaric, M. (2017). Dicamba spray drift as influenced by wind speed and nozzle type. *Weed Technology*, *31*(5), 724–731. https://doi.org/10.1017/wet.2017.61

ASABE. (2020). *Spray nozzle classification by droplet spectra* (Standard 572.3). ASABE.

Azimi, A. H., Carpenter, T. G., & Reichard, D. L. (1985). Nozzle spray distribution for pesticide application. *Transactions of the ASAE*, *28*(5), 1410–1414. https://doi.org/10.13031/2013.32451

Bae, Y., & Koo, Y. M. (2013). Flight attitudes and spray patterns of a roll-balanced agricultural unmanned helicopter. *Applied Engineering in Agriculture*, *29*(5), 675–682.

Bode, L. E., Butler, B. J., & Goering, C. E. (1976). Spray drift and recovery as affected by spray thickener, nozzle type, and nozzle pressure. *Transactions of the ASAE*, *19*(2), 213–0218. https://doi.org/10.13031/2013.35997

Brewer, J. R., Willis, J., Rana, S. S., & Askew, S. D. (2017). Response of six turfgrass species and four weeds to three HPPD-inhibiting herbicides. *Agronomy Journal*, *109*(4), 1777–1784. https://doi.org/10.2134/agronj2016.06.0345

Brosnan, J. T., Breeden, G. K., & McCullough, P. E. (2010). Efficacy of two dithiopyr formulations for control of smooth crabgrass [*Digitaria ischaemum* (Schreb) Schreb. Ex Muhl.] at various stages of growth. *HortScience*, *45*(6), 961–965.

Brosnan, J. T., Breeden, G. K., Patton, A. J., & Weisenberger, D. V. (2013). Triclopyr reduces smooth crabgrass bleaching with topramezone without compromising efficacy. *Applied Turfgrass Science*, *10*(1), 1–3. https://doi.org/10.1094/ATS-2013-0038-BR

Butler, E. L., Galle, G. H., & Kerns, J. P. (2019). Influence of nitrogen rate and timing, fungicide application method, and simulated rainfall after fungicide application on brown patch severity in tall fescue. *Crop, Forage & Turfgrass Management*, *5*(1), 1–6.

Butler Ellis, M., Swan, T., Miller, P. C. H., Waddelow, S., Bradley, A., & Tuck, C. R. (2002). PM—Power and machinery: Design factors affecting spray characteristics and drift performance of air induction nozzles. *Biosystems Engineering*, *82*(3), 289–296. https://doi.org/10.1006/bioe.2002.0069

Cardina, J., Johnson, G. A., & Sparrow, D. H. (1997). The nature and consequence of weed spatial distribution. *Weed Science*, *45*(3), 364–373. https://doi.org/10.1017/S0043174500092997

Cunha, M., Carvalho, C., & Marcal, A. R. (2012). Assessing the ability of image processing software to analyse spray quality on water-sensitive papers used as artificial targets. *Biosystems Engineering*, *111*(1), 11–23. https://doi.org/10.1016/j.biosystemseng.2011.10.002

Debouche, C., Huyghebaert, B., & Mostade, O. (2000). Simulated and measured coefficients of variation for the spray distribution under a static spray boom. *Journal of Agricultural Engineering Research*, *76*(4), 381–388. https://doi.org/10.1006/jaer.2000.0552

Dernoeden, P. H. (2001). Reduced herbicide rates for smooth crabgrass control in the Mid-Atlantic region. *International Turfgrass Society Research Journal*, *9*, 1005–1008.

Dernoeden, P. H., Bigelow, C. A., Kaminski, J. E., & Krouse, J. M. (2003). Smooth crabgrass control in perennial ryegrass and creeping bentgrass tolerance to quinclorac. *HortScience*, *38*(4), 607–612. https://doi.org/10.21273/HORTSCI.38.4.607

DJI. (2018). *Agras MG-1P user manual*. DJI.

Elmore, M. T., Brosnan, J. T., Kopsell, D. A., & Breeden, G. K. (2012). Nitrogen-enhanced efficacy of mesotrione and topramezone for smooth crabgrass (*Digitaria ischaemum*) control. *Weed Science*, *60*(3), 480–485. https://doi.org/10.1614/WS-D-11-00169.1

Foqué, D., Pieters, J. G., & Nuyttens, D. (2012). Comparing spray gun and spray boom applications in two ivy crops with different crop densities. *HortScience*, *47*(1), 51–57. https://doi.org/10.21273/HORTSCI.47.1.51

Fritz, B. K., Gill, M. P., & Bretthauer, S. (2019). Examining aerial application swath pattern evaluations under in-wind and cross-wind conditions. In D. J. Linscott (Ed.) *Innovative formulation, application and adjuvant technologies for agriculture* (Vol. 39, pp. 24–38). ASTM International. http://doi.org/10.1520/STP161920180123

Fritz, B., & Martin, D. (2020). Measurement and analysis methods for determination of effective swath width from unmanned aerial vehicles. In *40th Symposium on pesticide formulation and delivery systems: Formulation, application and adjuvant innovation* (pp. 62–85). ASTM International.

Fritz, B. K., Hoffmann, W. C., Bagley, W. E., & Hewitt, A. (2011). Field scale evaluation of spray drift reduction technologies from ground and aerial application systems. *Journal of ASTM International*, *8*(5), 1–11. https://doi.org/10.1520/JAI103457

Grift, T. E., Walker, J. T., & Gardisser, D. R. (2000). Spread pattern analysis tool (SPAT): II. Examples of aircraft pattern analysis. *Transactions of the ASAE*, *43*(6), 1351–1362. https://doi.org/10.13031/2013.3032

Grisso, R. D., Askew, S. D., & McCall, D. S. (2019). *Nozzles: Selection and sizing* (Publication No. 442-032). Virginia Cooperative Extension, Virginia Tech.

Hunter, J. E., Gannon, T. W., Richardson, R. J., Yelverton, F. H., & Leon, R. G. (2020). Coverage and drift potential associated with nozzle and speed selection for herbicide applications using an unmanned aerial sprayer. *Weed Technology*, *34*(2), 235–240. https://doi.org/10.1017/wet.2019.101

ISO. (2015). *Crop protection equipment—Spray deposition test for field crop—Part 1: Measurement in a horizontal plane* (ISO standard 24253-1). ISO.

Knoche, M. (1994). Effect of droplet size and carrier volume on performance of foliage-applied herbicides. *Crop Protection*, *13*(3), 163–178. https://doi.org/10.1016/0261-2194(94)90075-2

Koo, D., Askew, S. D., Godara, N., & Peppers, J. M. (2023). Herbicides applied with an agricultural spray drone control smooth crabgrass in managed turf. In *Proceedings of the Southern Weed Science Society* (Vol. 76, p. 133). Southern Weed Science Society.

Koo, D., Askew, S. D., Henderson, C. A., Godara, N., Peppers, J., & Goncalves, C. G. (2022). Height and nozzle selection influence droplet vaporization from agricultural spray drones [Abstract]. *ASA, CSSA, SSSA International Annual Meeting, Baltimore, MD*. ASA-CSSA-SSSA. https://scisoc.confex.com/scisoc/2022am/meetingapp.cgi/Paper/142485

Koo, D., Gonçalves, C. G., & Askew, S. D. (2024). Agricultural spray drone deposition, Part 2: Operational height and nozzle influence pattern uniformity, drift, and weed control. *Weed Science*.

Langenakens, J., Vergauwe, G., & Moor, A. D. (2002). Comparing hand held spray guns and spray booms in lettuce crops in a greenhouse. *Aspects of Applied Biology*, *66*, 123–128.

Li, X., Giles, D. K., Andaloro, J. T., Long, R., Lang, E. B., Watson, L. J., & Qandah, I. (2021). Comparison of UAV and fixed-wing aerial application for alfalfa insect pest control: Evaluating efficacy, residues, and spray quality. *Pest Management Science*, *77*(11), 4980–4992. https://doi.org/10.1002/ps.6540

Li, X., Giles, D. K., Niederholzer, F. J., Andaloro, J. T., Lang, E. B., & Watson, L. J. (2021). Evaluation of an unmanned aerial vehicle as a new method of pesticide application for almond crop protection. *Pest Management Science*, *77*(1), 527–537. https://doi.org/10.1002/ps.6052

Martin, D. E., Woldt, W. E., & Latheef, M. A. (2019). Effect of application height and ground speed on spray pattern and droplet spectra from remotely piloted aerial application systems. *Drones*, *3*(4), 83. https://doi.org/10.3390/drones3040083

McIntosh, M. S. (1983). Analysis of combined experiments. *Agronomy Journal*, *75*(1), 153–155. https://doi.org/10.2134/agronj1983.00021962007500010041x

Miller, P. C. H., Ellis, M. B., Lane, A. G., O'sullivan, C. M., & Tuck, C. R. (2011). Methods for inimizing drift and off-target exposure from boom sprayer applications. *Aspects of Applied Biology*, *106*, 281–288.

Nordbo, E., Kristensen, K., & Kirknel, E. (1993). Effects of wind direction, wind speed and travel speed on spray deposition. *Pesticide Science*, *38*(1), 33–41. https://doi.org/10.1002/ps.2780380106

Ozkan, H. E., & Ackerman, K. D. (1992). An automated computerized spray pattern analysis system. *Applied Engineering in Agriculture*, *8*(3), 325–331. https://doi.org/10.13031/2013.26072

Panneton, B. (2002). Image analysis of water–sensitive cards for spray coverage experiments. *Applied Engineering in Agriculture*, *18*(2), 179. https://doi.org/10.13031/2013.7783

Parkin, C. S., & Wyatt, J. C. (1982). The determination of flight-lane separations for the aerial application of herbicides. *Crop Protection*, *1*(3), 309–321. https://doi.org/10.1016/0261-2194(82)90006-0

Patton, A. J., Weisenberger, D. V., Schortgen, G. P., Fausey, J. C., & Breuninger, J. M. (2018). Performance of postemergence broadleaf herbicides applied with novel lawn care application equipment. *Crop, Forage & Turfgrass Management*, *4*(1), 1–5.

Prairie Agricultural Machinery Institute. (1989). *Evaluation report 597*. Prairie Agricultural Machinery Institute.

Putri, A. D., Singh, V., de Castro, E. B., Rutland, C. A., McElroy, J. S., Tseng, T. M., & McCurdy, J. D. (2024). Confirmation and differential metabolism associated with quinclorac resistance in smooth crabgrass (*Digitaria ischaemum*). *Weed Science*, *72*, 1–30.

Qin, W. C., Qiu, B. J., Xue, X. Y., Chen, C., Xu, Z. F., & Zhou, Q. Q. (2016). Droplet deposition and control effect of insecticides sprayed with an unmanned aerial vehicle against plant hoppers. *Crop Protection*, *85*, 79–88. https://doi.org/10.1016/j.cropro.2016.03.018

Richardson, B., Kimberley, M. O., & Schou, W. C. (2004). Defining acceptable levels of herbicide deposit variation from aerial spraying. *Applied Engineering in Agriculture*, *20*(3), 259–267. https://doi.org/10.13031/2013.16059

Richardson, B., Rolando, C. A., Somchit, C., Dunker, C., Strand, T. M., & Kimberley, M. O. (2020). Swath pattern analysis from a multi-rotor unmanned aerial vehicle configured for pesticide application. *Pest Management Science*, *76*(4), 1282–1290. https://doi.org/10.1002/ps.5638

Richardson, R. G., Combellack, J. H., & Andrew, L. (1986). Evaluation of a spray nozzle patternator. *Crop Protection*, *5*(1), 8–11. https://doi.org/10.1016/0261-2194(86)90032-3

Salyani, M., & Fox, R. D. (1999). Evaluation of spray quality by oil and water-sensitive papers. *Transactions of the ASAE*, *42*(1), 37–43. https://doi.org/10.13031/2013.13206

Salyani, M., Zhu, H., Sweeb, R., & Pai, N. (2013). Assessment of spray distribution with water-sensitive paper. *Agricultural Engineering International: CIGR Journal*, *15*(2), 101–111.

Sánchez-Hermosilla, J., Rincón, V. J., Páez, F., Agüera, F., & Carvajal, F. (2011). Field evaluation of a self-propelled sprayer and effects of the application rate on spray deposition and losses to the ground in greenhouse tomato crops. *Pest Management Science*, *67*(8), 942–947. https://doi.org/10.1002/ps.2135

Shepard, D., Agnew, M., Fidanza, M., Kaminski, J., & Dant, L. (2006). Selecting nozzles for fungicide spray applications. *Golf Course Management*, *74*, 83–88.

Solie, J. B., & Gerling, J. F. (1985). Spray pattern analysis system for pesticide application. *Transactions of the ASAE*, *28*(5), 1430–1434. https://doi.org/10.13031/2013.32455

Spraying Systems Co. (2023). *TeeJet technologies catalog 52*. Spraying Systems Co.

Stainier, C., Destain, M. F., Schiffers, B., & Lebeau, F. (2006). Droplet size spectra and drift effect of two phenmedipham formulations and four adjuvants mixtures. *Crop Protection*, *25*(12), 1238–1243. https://doi.org/10.1016/j.cropro.2006.03.006

Sumner, P. E. (2012). *Sprayer nozzle selection* (Bulletin No. 1158). University of Georgia.

Taylor, W. A., Womac, A. R., Miller, P. C. H., & Taylor, B. P. (2004). An attempt to relate drop size to drift risk. In *Proceedings of the International Conference on Pesticide Application for Drift Management* (pp. 210–223). Washington State University.

Teske, M. E., Wachspress, D. A., & Thistle, H. W. (2018). Prediction of aerial spray release from UAVs. *Transactions of the ASABE*, *61*(3), 909–918. https://doi.org/10.13031/trans.12701

Thornton, M. E., & Kibble-White, R. (1974). Apparatus used for spray nozzle evaluation at the Weed Research Organization. *PANS Pest Articles & News Summaries*, *20*(4), 465–475.

Wang, G., Han, Y., Li, X., Andaloro, J., Chen, P., Hoffmann, W. C., Han, X., Chen, S., & Lan, Y. (2020). Field evaluation of spray drift and environmental impact using an agricultural unmanned aerial vehicle (ASD) sprayer. *Science of the Total Environment*, *737*, 139793. https://doi.org/10.1016/j.scitotenv.2020.139793

Wang, G., Lan, Y., Qi, H., Chen, P., Hewitt, A., & Han, Y. (2019). Field evaluation of an unmanned aerial vehicle (UAV) sprayer: Effect of spray volume on deposition and the control of pests and disease in wheat. *Pest Management Science*, *75*(6), 1546–1555. https://doi.org/10.1002/ps.5321

Wen, Y., Zhang, R., Chen, L., Huang, Y., Yi, T., Xu, G., Li, L., & Hewitt, A. J. (2019). A new spray deposition pattern measurement system based on spectral analysis of a fluorescent tracer. *Computers and Electronics in Agriculture*, *160*, 14–22. https://doi.org/10.1016/j.compag.2019.03.008

How to cite this article: Koo, D., Godara, N., Cubas, J. R. R., & Askew, S. D. (2025). A method to spatially assess multipass spray deposition patterns via UV fluorescence and weed population shifts. *Crop Science*, *65*, e21377. https://doi.org/10.1002/csc2.21377